NJC

PAPER

View Article Online
View Journal | View Issue

Cite this: *New J. Chem.*, 2014, **38**, 2813

Theoretical investigation of atmospheric chemistry of volatile anaesthetic sevoflurane: reactions with the OH radicals and atmospheric fate of the alkoxy radical $(CF_3)_2CHOCHFO$: thermal decomposition *vs.* oxidation†

Bhupesh Kumar Mishra,[a] Makroni Lily,[b] Arup Kumar Chakrabartty,[a] Debajyoti Bhattacharjee,[a] Ramesh Chandra Deka*[a] and Asit K. Chandra*[b]

Received (in Montpellier, France) 13th November 2013, Accepted 26th March 2014

DOI: 10.1039/c3nj01408h

www.rsc.org/njc

A theoretical study on the mechanism and kinetics of the gas phase reactions of a volatile anaesthetic compound $(CF_3)_2CHOCH_2F$ (Sevoflurane) with the OH radicals has been carried out using the hybrid HF–density functional M06-2X/6-31+G(d,p) method. Three conformations are predicted for the Sevoflurane molecule. Among the three conformers, the most stable one is considered for a detailed study. Reaction profiles are modeled including the formation of pre-reactive and post-reactive complexes at entrance and exit channels. Single point energy calculations have been performed by using the 6-311++G(d,p) basis set. The hydrogen abstraction from the $-CH_2F$ group is found to be the dominant reaction channel for hydrogen abstraction by OH radicals. Theoretically the calculated rate constant is found to be in good agreement with the experimentally measured ones. Using group-balanced isodesmic reactions, the standard enthalpies of formation for $(CF_3)_2CHOCH_2F$, $(CF_3)_2COCH_2F$ and $(CF_3)_2CHOCHF$ radicals are also reported for the first time. The atmospheric fate of the alkoxy radical, $(CF_3)_2CHOCHFO$, is also investigated for the first time using the same level of theory. Out of four prominent plausible decomposition channels including oxidation, our results clearly point out that reaction with O_2 is the dominant path for the decomposition of $(CF_3)_2CHOCHFO$ in the atmosphere involving the lowest energy barrier which is in accord with recent experimental findings.

I Introduction

It is now well recognized fact that atomic chlorine transported to the stratosphere on account of release of a variety of chlorine containing compounds, particularly chlorofluorocarbon (CFC), is responsible for the catalytic destruction of ozone in the atmosphere.[1,2] Recently, hydrofluoroether (HFE) and hydrochloroether (HCE) have been the focus of intense attention as replacement materials for CFC and hydrochlorofluorocarbon (HCFC) in applications such as heat-transfer fluids in refrigeration systems, cleaning agents in electronic industry, foam-blowing agents and also for lubricant deposition.[3,4] The absence of chlorine atoms in HFEs shows that such compounds would have little impact on the stratospheric ozone and that they possess a negligible ozone depleting potential (ODP).[5] In recent times, some non-segregated HFE have been used to serve as a model complex for the anaesthetic gases[6,7] to replace ethers containing Cl and/or Br atoms. For example, desflurane ($CHF_2OCHFCF_3$) and Sevoflurane [$(CF_3)_2CHOCH_2F$] are two of the most common volatile anaesthetic agents, and have replaced others such as isoflurane ($CF_3CHClOCHCF_2$), halothane ($CF_3CHClBr$) and enflurane (CHF_2OCF_2CHFCl). The total amount of these compounds used globally has been estimated to be in the order of 10 kilotons per year.[8] Segregated hydrofluoroethers are ethers with fluorocarbon on one side of the oxygen atom and hydrocarbon on the other, for example, $C_4F_9OCH_3$ (HFE-7100), $C_4F_9OC_2H_5$ (HFE-7200) and $C_7F_{15}OC_2H_5$ (HFE-7500). Non-segregated HFEs may have both hydrogen and fluorine on one or both sides of the oxygen. For *e.g.*; $C_4F_9OC_2F_4H$, $C_6F_{13}OCF_2H$, $HC_3F_6OC_3F_6H$, $C_3F_7OCH_2F$, $HCF_2OCF_2OCF_2H$, $HCF_2OCF_2CF_2OCF_2H$, $HC_3F_6OCH_3$, $HCF_2OCF_2OC_2F_4OCF_2H$ are a class of non-segregated HFEs.

[a] *Department of Chemical Sciences, Tezpur University Tezpur, Assam, 784 028, India. E-mail: ramesh@tezu.ernet.in; Fax: +91 3712267005; Tel: +91 3712267008*
[b] *Department of Chemistry, North-Eastern Hill University, Shillong, 793 022, India. E-mail: akchandra@nehu.ac.in; Fax: +91 3642550486; Tel: +91 3642722622*

† Electronic supplementary information (ESI) available. See DOI: 10.1039/c3nj01408h

It is well known that more than 80% of inhalation anaesthetic agent is exhaled unchanged by the patient and therefore emitted into the lower atmosphere.[9] The major atmospheric effects that may arise from emission of the volatile anaesthetic are their contribution to ozone depletion in the stratosphere and to green house warming in the troposphere. Hence, there is a particular need to investigate the atmospheric chemistry of these compounds in order to determine their atmospheric impact. Therefore, several studies have focused on the impact of these anaesthetic agents on the environment to determine the most environmentally compatible anaesthetic.[9–13] Very recently, Bravo *et al.*[14] used smog chamber/Gas Chromatography techniques to investigate the atmospheric degradation of fluroxene, an inhalational anaesthetic, through oxidation with OH and Cl radicals at 298 K and atmospheric pressure. Zierkiewicz[15] theoretically investigated the mechanism of the reaction between desflurane ($CF_3CHFOCHF_2$) and Cl atom at the CCSD(T)/CBS level of theory.

The reaction of Sevoflurane with OH radicals was first studied by Brown *et al.*[16] in 1989 and they reported a rate constant of $(7.3 \pm 2.2) \times 10^{-14}$ cm^3 molecule^{-1} s^{-1} at 299 K. Subsequently, Langbein *et al.*[8] performed another experimental study by using a relative method and they reported a significantly lower rate constant value of $(2.7 \pm 0.5) \times 10^{-14}$ cm^3 molecule^{-1} s^{-1} at 298 K. Recently, this reaction has been studied experimentally by Andersen *et al.*[17] using a smog chamber and the FTIR technique. The experimental rate constant was derived as k(OH + $(CF_3)_2CHOCH_2F$) = $(3.9 \pm 0.3) \times 10^{-14}$ cm^3 molecule^{-1} s^{-1} at 298 K. In other reports, Chen *et al.*[18] studied the kinetics of the reactions of OH radicals with a similar HFE, $(CF_3)_2CHOCH_3$, using a smog chamber and the FTIR technique at 298 ± 2 K and atmospheric pressure (760 ± 10 Torr). The atmospheric lifetime of Sevoflurane with OH radicals has been estimated to be 1.8 years.[12] However, the total lifetime (including OH reaction, ocean loss and stratospheric loss) of Sevoflurane has been reported to be 2.2 years.[19,20] Moreover, experimental studies provided only the total rate constant and it is difficult to predict the detailed mechanism, thermochemistry and contribution of each reaction channel towards the overall rate constant. Thus, for better understanding of mechanistic pathways, kinetics and thermo chemistry we must rely on quantum chemical methods. In the present work, we have investigated the hydrogen abstraction reactions between Sevoflurane and OH radicals at the DFT level. To the best of our knowledge, this is the first detailed theoretical study of the above-mentioned H-abstraction reactions of Sevoflurane with OH radicals. Our calculation indicates that three reaction channels, one from the –$CH(CF_3)_2$ group (−CH attached to two $-CF_3$ groups) and two reaction channels from the –CH_2F group are feasible for the $(CF_3)_2CHOCH_2F$ + OH reactions as given below:

$$(CF_3)_2CHOCH_2F + OH \rightarrow (CF_3)_2COCH_2F + H_2O \quad (1)$$

$$(CF_3)_2CHOCH_2F + OH \rightarrow (CF_3)_2CHOCHF + H_2O \quad (2a \text{ \& } b)$$

A general mechanism of OH-initiated tropospheric degradation of Sevoflurane ($(CF_3)_2CHOCH_2F$) is shown in Scheme 1 leading to the formation of the haloalkoxy radical ($(CF_3)_2CHOCHFO$). The

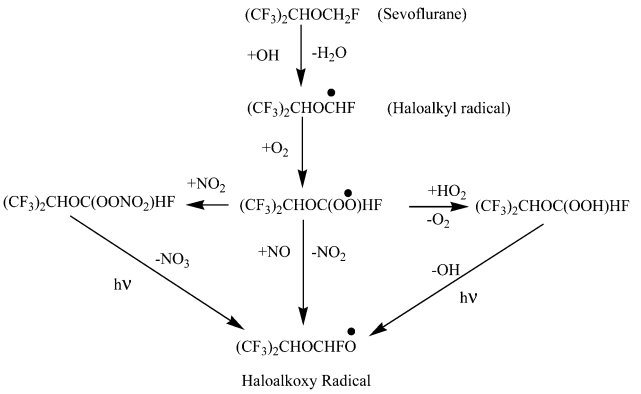

Scheme 1 Tropospheric degradation of Sevoflurane initiated by OH radicals.

chemistry of haloalkoxy radicals has been a subject of extensive experimental and theoretical investigations as these species are interesting intermediates in the atmospheric oxidation of halogenated hydrocarbons.[21–26] Due to the significant role played by haloalkoxy radicals formed in the destruction of a variety of organic compounds released into the atmosphere, studying the fate of $(CF_3)_2CHOCHFO$ formed from Sevoflurane is needed from the viewpoint of understanding its role in the atmospheric chemistry. To the best of our knowledge, no theoretical study has been carried out to elucidate the dissociative pathways of the $(CF_3)_2CHOCHFO$ radical derived from one of the important classes of anaesthetic agent, Sevoflurane. Thus, there is a desirable need to perform quantum mechanical calculations to determine the energetics involved during the decomposition of the $(CF_3)_2CHOCHFO$ radical.

There are four potential pathways of decomposition of the $(CF_3)_2CHOCHFO$ radical produced from Sevoflurane that involve bond scission and oxidation processes. These are represented as follows:

$$(CF_3)_2CHOCHFO \rightarrow (CF_3)_2CHO + CHFO \quad (3)$$

$$\rightarrow (CF_3)_2CHOCHO + F \quad (4)$$

$$\rightarrow (CF_3)_2CHOCFO + H \quad (5)$$

$$+ O_2 \rightarrow (CF_3)_2CHOCFO + HO_2 \quad (6)$$

The thermochemical studies have been carried out to analyze the stability of all the species involved in the reactions. To have a clear picture of the total reaction mechanism, we have treated the whole reaction step by step. In addition, the knowledge of accurate enthalpy of formation ($\Delta_f H^\circ_{298}$) for $(CF_3)_2CHOCH_2F$ and radicals generated, $(CF_3)_2COCH_2F$ and $(CF_3)_2CHOCHF$, is of vital importance for determining the thermodynamic properties and the kinetics of the atmospheric process. However, no theoretical or experimental study on standard enthalpy of formation has been reported so far for these species. Here, we predict the enthalpies of formation using isodesmic reactions at the M06-2X/6-31+G(d,p) level.

II Computational methods

Electronic structure calculations were performed using the Gaussian 09 suite of program.[27] The geometries of all molecular species involved in this study are fully optimized by employing the density functional M06-2X[28] method in conjunction with the 6-31+G(d,p) basis set for all the elements. Zhao and Truhlar[28] recently developed the M06 family of local (M06-L) and hybrid (M06, M06-2X) meta-GGA functionals that show promising performance in the kinetic and thermodynamic calculations without the need of refining the energies by post Hartree–Fock methods, and these functionals have been applied successfully in the recent studies.[29–35] The formation of pre- and post-reactive complexes along the entry and exit of each reaction channel has been observed. Hessian calculations for obtaining the vibrational frequencies were performed at the same level of theory as that for the geometry optimization to check whether the optimized geometrical structure is an energy minimum (with no imaginary frequency) or TS (with one and only one imaginary frequency). To ascertain that the identified transition states connect reactants and products smoothly, intrinsic reaction coordinate (IRC) calculations[36] were also performed at the M06-2X/6-31+G(d,p) level. To obtain more accurate energies and barrier heights, the energies are further refined by using Pople's split-valence triple-ζ quality 6-311++G(d,p) basis set based on M06-2X/6-31+G(d,p) optimized geometries.

III Results and discussion

A. Structure and energetics

The conformational landscape of Sevoflurane was recently investigated by Freitas *et al.*,[37] Lesarri *et al.*[38] and Tang *et al.*[39] by means of experimental and theoretical tools. We have chosen the lowest energy conformer (SC1) for the present study since the population of other conformers is likely to be small at normal temperature. The optimized structure of the lowest energy conformer is shown in Fig. 1. Our resulted geometrical parameters for SC1 are in reasonable agreement with the values calculated at the B3LYP/6-311 + G(2d, p) level by Tang *et al.*[39] and Singh *et al.*[40] The bond distances of the optimized structure of Sevoflurane calculated in the present study are also close to the average bond distance values taken from CRC Handbook of Physics and Chemistry reported by Tang *et al.*[39] The calculated enthalpy of reactions ($\Delta_r H^o$) at 298 K for the reaction of $(CF_3)_2CHOCH_2F$ with OH radicals are recorded in Table 1. Thermal corrections to the energy at 298 K were included in the determination of these thermodynamic quantities. The reaction enthalpy ($\Delta_r H^o$) values for reactions (1–2) as given in Table 1 show that all reaction channels are significantly exothermic in nature and thus thermodynamically facile.

There are two potential hydrogen abstraction sites of $(CF_3)_2CHOCH_2F$ namely the $-CH(CF_3)_2$ group and the $-CH_2F$ group. However, as can be seen from the geometrical parameters and stereographical orientation the hydrogen atoms in the $-CH_2F$ group are not equivalent. One H-atom is different from the other two in the $-CH_2F$ group. Three transition states (TS) are therefore located for the reactions $(CF_3)_2CHOCH_2F$ + OH; one TS (TS1) for H-abstraction from the $-CH(CF_3)_2$ group and two TSs for the same from the $-CH_2F$ group (TS2a and TS2b). Therefore three H-abstraction reaction channels exist for the reactions studied here.

In the entrance channels, the pre-reactive complex has been validated in the present work and designated by prefix RC followed by a number. In the exit channels, there are also product complexes occurring before the release of the final

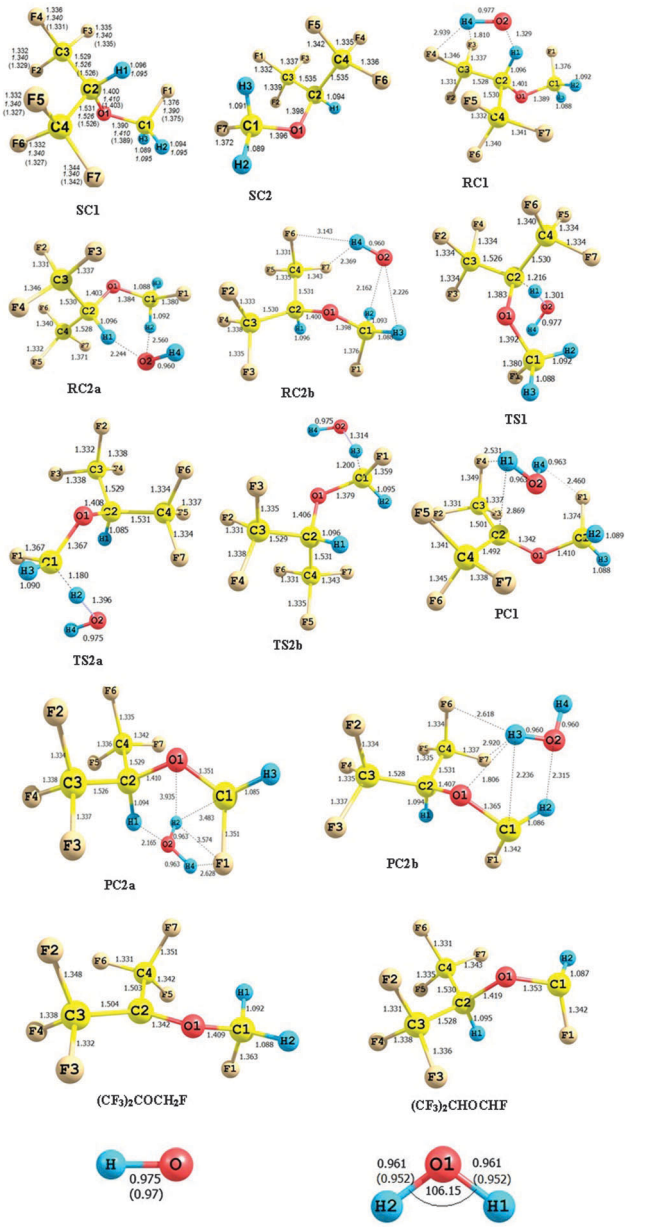

Fig. 1 Optimized geometries of reactants, reactant complexes, transition states, product complexes and products involved in the H-atom abstraction reactions of Sevoflurane by OH radicals at the M06-2X/6-31+G(d,p) level. Bond lengths are in angstroms. The italic values and values in parenthesis are taken from ref. 38 and 39, respectively.

Table 1 Reaction enthalpy ($\Delta_r H^\circ_{298}$) for reaction channels (1–2) and enthalpies of formation ($\Delta_f H^\circ_{298}$) for species at 298 K. All values are in kcal mol^{-1}

		M06-2X/6-311++G(d,p)
$\Delta_r H^\circ_{298}$		
Reaction 1		−16.28
Reaction 2		−16.49
Species	**Isodesmic reactions**	**M06-2X/6-311++G(d,p)**
$\Delta_f H^\circ_{298}$		
$(CF_3)_2CHOCH_2F$	7	−415.49
	8	−414.13
Average		−414.81
$(CF_3)_2COCH_2F$		−364.36
$(CF_3)_2CHOCHF$		−364.57

products, which are labeled with the prefix PC and a number to follow. The optimized geometries of reactants, reactant complexes, transition states, product complexes and products along with structural parameters obtained at the M06-2X/6-31+G(d,p) level are shown in Fig. 1. On the reactant side of reaction channels (1–2) three hydrogen-bonded complexes (RC1, RC2a and RC2b) are located. In complexes RC1, RC2a and RC2b, hydrogen bonding interactions can be found from the interatomic distances as shown in Fig. 1. At the same time, the product complexes (PC1, PC2a and PC2b) with energies less than the corresponding products are located at the exits of the two reaction channels. So it is clear that all the reaction channels (1–2) may proceed *via* indirect mechanisms. The search was made along the minimum energy path on a relaxed potential energy surface. Visualization of the optimized geometries reveals that the breaking C–H bond and the forming O···H bond in TS1 are, respectively, 16.33% and 35.37% longer than the C–H bond length in $(CF_3)_2CHOCH_2F$ and in H_2O, whereas the same values amount to 07.86% and 45.26% for TS2a. While for the transition states TS2b, the elongations of the breaking C–H bonds are found to be 10.20% and 36.73%. These values indicate that the reactions (1–2) proceed *via* an early transition state structure expected for an exothermic hydrogen abstraction reaction.

Harmonic vibrational frequencies of all the stationary points involved in reactions (1–2) are listed in Table S1 in the ESI.† All the reactants, reactant complexes, product complexes and products were identified with all positive frequencies while each transition state was characterized by only one imaginary frequency. The imaginary frequency values for TS1, TS2a and TS2b are 2118*i*, 1822*i* and 1370*i* cm^{-1}, respectively. Intrinsic reaction coordinate (IRC)[31] calculations have also been performed for each transition state at the same level of theory using the Gonzalez–Schlegel steepest descent path in the mass-weighted Cartesian coordinates with a step size of 0.01 (amu$^{1/2}$ bohr). The IRC plots for transition states reveal that the transition state structures smoothly connect the reactant and the product sides.

The relative energies including ZPE for all species and transition states involved in reactions (1–2) calculated at the M06-2X/6-311++G(d,p) level are presented in Table S2 in the ESI.† The calculated barrier heights at the M06-2X/6-311++G(d,p) level for TS1, TS2a and TS2b are 1.52, 1.42 and 3.50 kcal mol^{-1}, respectively. The barrier height values show that hydrogen abstraction by OH radicals from the terminal $-CH_2F$ group is more facile than that from the –CH attached to two $-CF_3$ groups. This finding contradicts with the observation of Chen *et al.*[18] that the CH attached to two $-CF_3$ groups is more reactive than the terminal $-CH_3$ towards hydrogen abstraction reactions by the OH radical in a similar compound, $(CF_3)_2CHOCH_3$.

Literature survey reveals that there is no experimental data available for the comparison of the energy barrier for the H-atom abstraction reaction of $(CF_3)_2CHOCH_2F$ by OH radicals. However, in order to ascertain the reliability of the calculated barrier height values, we compared our results with the values calculated by Singh *et al.*[40] for the H-atom abstraction reaction from –CHO and $-CH_2F$ sites in $(CF_3)_2CHOCH_2F$ + Cl reactions. The optimized geometries of two transition states (TS7 and TS8) are given in Fig. S1 in ESI.† Our calculated barrier heights amount to 8.70 and 3.63 kcal mol^{-1} at the M06-2X/6-311++G(d,p) level of theory for –CHO and $-CH_2F$ sites, respectively, whereas the same obtained from the M06-2X/6-31+G(d,p) calculations amount to 8.60 and 3.51 kcal mol^{-1}. Our calculated barrier heights at both levels are in excellent agreement with the reported values of 8.8 and 3.4 kcal mol^{-1} at the CCSD(T)/6-311G(d,p) level of theory by Singh *et al.*[40] Thus, the calculated energy barriers for the title reactions studied here at M06-2X/6-311++G(d,p) can be relied upon. This gives us a confidence that the energy barrier calculated using the M06-2X/6-311++G(d,p) method on the geometries optimized at M06-2X/6-31+G(d,p) yields reliable values for the hydrogen abstraction channels considered in the present study.

The schematic potential energy profile of $(CF_3)_2CHOCH_2F$ + OH reactions obtained at the M06-2X/6-311++G(d,p)//M06-2X/6-31+G(d,p) level with ZPE corrections is shown in Fig. 2. In the construction of the energy diagram, zero-point energy corrected

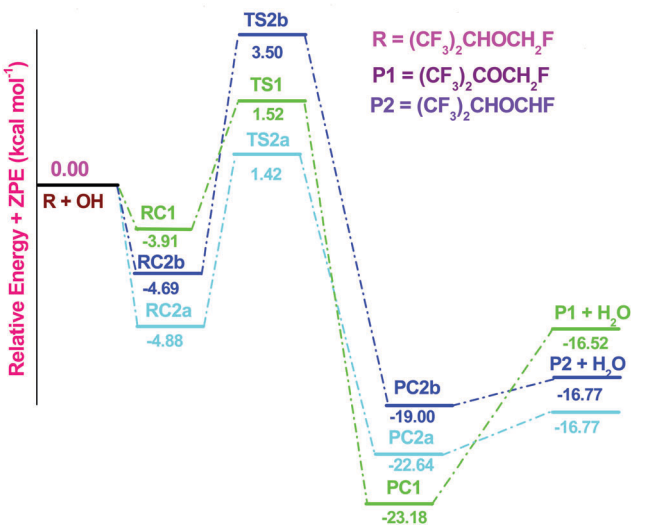

Fig. 2 Schematic potential energy diagram for the $(CF_3)_2CHOCH_2F$ + OH reactions. Relative energies (in kcal mol^{-1}) are calculated at the M06-2X/6-311++G(d,p) + ZPE level.

Table 2 Bond dissociation energy (D^0_{298}) calculated at different levels of theory. All values are in kcal mol^{-1}

Bond dissociation type	M06-2X/ 6-311++G(d,p)	BHandHLYP/ 6-311G(d,p)	MPWB1K/ 6-31+G(d,p)
C–H bond			
$(CF_3)_2CHOCH_2F \rightarrow (CF_3)_2COCH_2F + H$	102.59	102.95	103.71
$(CF_3)_2CHOCH_2F \rightarrow (CF_3)_2CHOCHF + H$	102.38	100.37	101.72

relative energies as recorded in Table S2 in ESI† are utilized. These energies are plotted with respect to the ground state energy of $(CF_3)_2CHOCH_2F$ + OH arbitrarily taken as zero. Spin contamination is not important for the open shell radicals involved in $(CF_3)_2CHOCH_2F$ + OH reactions because $<S^2>$ is found to be 0.76 at M06-2X/6-31+G(d,p) before annihilation that is only slightly larger than the expected value of $<S^2>$ = 0.75 for doublets.

The calculated bond-dissociation energies, BDE (D^0_{298}), of the C–H bonds of the $(CF_3)_2CHOCH_2F$ molecule are given in Table 2. The D^0_{298} values obtained from M06-2X/6-311++G(d,p) results amount to 102.59 and 102.38 kcal mol^{-1}, respectively. Moreover, our calculated (D^0_{298}) values for the C–H bonds is found to be somewhat higher than that of 98.4 and 97.7 kcal mol^{-1}, respectively, for –CHO and –CH_2F sites of $(CF_3)_2CHOCH_2F$ reported by Singh *et al.*[40] To check whether this is an artifact of our calculation, we have also calculated D^0_{298} values using MPWB1K/6-31+G(d,p) and BHandHLYP/6-311G(d,p) methods and the results are recorded in Table 2. From Table 2, it is seen that the calculated BDE values at MPWB1K/6-31+G(d,p) and BHandHLYP/6-311G(d,p) levels are found to be in good agreement with the values obtained at the M06-2X/6-31++G(d,p) level of theory. This reveals that our calculated D^0_{298} values at the M06-2X level are reliable. Recently, it has been reported that this functional (M06-2X) yields reliable results for bond dissociation enthalpies.[41–44] However, our calculated D^0_{298} value for the C–H bond in the –$CH(CF_3)_2$ group (102.59 kcal mol^{-1}) of $(CF_3)_2CHOCH_2F$ is in reasonable agreement with the reported D^0_{298} value for the C–H bond in the –$CH(CF_3)_2$ group (99.4 kcal mol^{-1}) of $(CF_3)_2CHOCH_3$ reported by Devi and Chandra.[45]

The standard enthalpy of formation ($\Delta_fH^o_{298}$) at 298 K for $(CF_3)_2CHOCH_2F$ and the radicals generated from hydrogen abstraction, $(CF_3)_2COCH_2F$ and $(CF_3)_2CHOCHF$, can provide valuable information for understanding the mechanism and thermochemical properties of their reactions and most importantly for atmospheric modeling, but these values are not yet reported. The group-balanced isodesmic reactions, in which the number and types of bonds are conserved, are used as working chemical reactions herein to calculate the $\Delta_fH^o_{298}$ for $(CF_3)_2CHOCH_2F$ and radicals generated from hydrogen abstraction reactions. Here, the following isodesmic reactions are used to estimate the enthalpies of formation of these species:

$$(CF_3)_2CHOCH_2F + CH_4 + CH_3F \rightarrow CF_3CH_2CF_3 + CH_3OCH_3 + CH_2F_2 \quad (7)$$

$$(CF_3)_2CHOCH_2F + CH_4 \rightarrow (CF_3)_2CHOCH_3 + CH_3F \quad (8)$$

All geometrical parameters of the species involved in the isodesmic reactions (7–8) were optimized at the M06-2X/6-31+G(d,p) level and energies of the species were then refined at the M06-2X/6-311++G(d,p) level of theory. At first we have calculated the reaction enthalpies ($\Delta_rH^o_{298}$) of the isodesmic reactions (7–8) as mentioned above using total energies of the species obtained at different levels including thermal correction to enthalpy estimated at the M06-2X/6-31+G(d,p) level. Since the $\Delta_rH^o_{298}$ value corresponds to the difference of the enthalpy of formation ($\Delta_fH^o_{298}$) values between the products and the reactants, the $\Delta_fH^o_{298}$ values of the reactant and product species can be easily evaluated by combining them with the known enthalpies of formation of the reference compounds involved in our isodesmic reaction schemes. The experimental $\Delta_fH^o_{298}$ values for CH_4: −17.89 kcal mol^{-1}, CH_3OCH_3: −44.08 kcal mol^{-1}, CH_3F: −55.99 kcal mol^{-1}, and CH_2F_2: −107.71 kcal mol^{-1} were taken from ref. 46 and that for $CF_3CH_2CF_3$: −336.50 kcal mol^{-1} and $(CF_3)_2CHOCH_3$: −364.20 kcal mol^{-1} were taken from ref. 45 and 47, respectively, to evaluate enthalpies of formation. The calculated values of enthalpies of formation are listed in Table 1. As can be seen from Table 1, the values of $\Delta_fH^o_{298}$ for the species obtained from the two isodesmic reactions at the two levels of theories are very consistent with each other. The average $\Delta_rH^o_{298}$ values obtained from our calculations for $(CF_3)_2CHOCH_2F$ is −414.81 kcal mol^{-1} at M06-2X/6-311++G(d,p). The $\Delta_rH^o_{298}$ values for $(CF_3)_2COCH_2F$ and $(CF_3)_2CHOCHF$ radicals can also be easily calculated from the reported $\Delta_rH^o_{298}$ values for reactions (1–2) as reported in Table 1, the calculated $\Delta_fH^o_{298}$ value for $(CF_3)_2CHOCH_2F$ and the experimental $\Delta_fH^o_{298}$ values for H_2O (−57.8 kcal mol^{-1}) and the OH (8.93 kcal mol^{-1}) radical.[48] The $\Delta_rH^o_{298}$ values for $(CF_3)_2COCH_2F$ and $(CF_3)_2CHOCHF$ radicals calculated from M06-2X/6-311++G(d,p) amounts to −364.36 and −364.57 kcal mol^{-1}, respectively. Moreover, because of the lack of the experimental values for the $\Delta_fH^o_{298}$ of the species involved in the title reactions, it is difficult to make a direct comparison between theoretical and experimental enthalpy of formation.

B. Atmospheric fate of the alkoxy radical

The fate of the fluoroalkoxy radical $(CF_3)_2CHOCHFO$ produced during its thermal decomposition in the atmosphere is envisaged to occur *via* reactions (3–6). The detailed thermodynamic calculations performed at the M06-2X/6-31+G(d,p) level for reaction enthalpies ($\Delta_rH^o_{298}$), free energies ($\Delta_rG^o_{298}$) and free energies of activation ($\Delta G^{\#}$), associated with reaction channels (3–6), are listed in Table S4 in ESI.† Results show that reaction channel (6) proceeds with an exothermicity of 41.48 kcal mol^{-1} along with a negative free energy change of 42.74 kcal mol^{-1}. This envisages that reaction channel (6) is thermodynamically the most favorable decomposition channel in comparison to reaction channels (3)–(5). Optimized geometries of reactants, products and transition states obtained at the M06-2X/6-31+G(d,p) level are shown in Fig. S1 in ESI.† Transition states obtained on the potential energy surfaces of reactions (3–6) are characterized as TS3, TS4, TS5 and TS6, respectively. The search

was made along the minimum energy path on a relaxed potential energy surface. The geometrical parameters of the optimized structure of each species involved in reactions (3–6) are listed in Fig. S1 in ESI.† In the optimized structure of TS3 the elongation of the C–O bond (C1–O1) is found to be 1.391 to 1.791 Å (about 28% increases) with a simultaneous shrinkage of the C1–O2 bond. This decrease has been found to be almost 8% (1.334 to 1.229 Å). Similar analysis made on the optimized structure of TS4 reveals the elongation of the C1–F1 bond length from 1.373 to 1.883 Å resulting in an increase of about 37% accompanied with a shrinkage of the C–O bond (C1–O2) 1.334 to 1.241 (~7%). The cleavage of the C–H bond (channel 7) leads to atomic hydrogen and $(CF_3)_2CHOCFO$ and the corresponding transition state TS5 shows major structural changes *i.e.*, a substantial elongation (45%) in the C1–H2 bond and a shortening (~11%) of the C–O bond (C1–O2). Similarly the results obtained for the optimized structure TS6 for reaction with O_2 reveal that the C–H bond (C1–H2) increases from 1.107 to 1.270 Å (approx. 14%).

Harmonic vibrational frequencies for reactants, products and transition states involved in reactions (3–6) are recorded in Table S5 in ESI.† These results show that the reactants and products have stable minima on their potential energy surface characterized by the occurrence of only real and positive vibrational frequencies. On the other hand, transition states are characterized by the occurrence of only one imaginary frequency obtained at 673*i*, 564*i*, 1087*i* and 1128*i* cm^{-1} for TS3, TS4, TS5 and TS6, respectively. Visualization of the listed imaginary frequencies gives a qualitative confirmation of the existence of transition states connecting reactant and products. The existence of the correct transition state on the potential energy surface, however, is ascertained by intrinsic reaction coordinate (IRC) calculation[31] performed at the same level of theory. The associated energy barriers corresponding to reactions (3–6) are recorded in Table S5 in ESI.† No experimental or theoretical data are available in the literature to compare the energy barriers associated with the decomposition channels of $(CF_3)_2CHOCHFO$ considered in the present investigation. The zero-point corrected total energies are used relative to the ground state energy of $(CF_3)_2CHOCHFO$ taken as zero and an energy diagram is constructed as shown in Fig. 3. The barrier height for reaction with O_2 is considerably lower than that for other decomposition pathways and the dominance of the oxidative pathways of this alkoxy radical in the atmosphere is thus envisioned which is in good agreement with the experimental findings of Andersen *et al.*[17]

C. Rate constant calculations

The rate constant for reactions (1–2) is calculated using Canonical Transition State Theory (CTST)[49] that involves a semi-classical one-dimensional multiplicative tunneling correction factor given by the following expression:

$$k(T) = \sigma\Gamma(T)\frac{k_B T}{h}\frac{Q_{TS}}{Q_A \cdot Q_B}\exp\frac{-\Delta E}{RT} \quad (9)$$

where, σ is the degeneracy of each reaction channel, $\Gamma(T)$ is the tunneling correction factor at temperature T. Q_{TS}, Q_A and Q_B are the total partition functions for the transition states and reactants

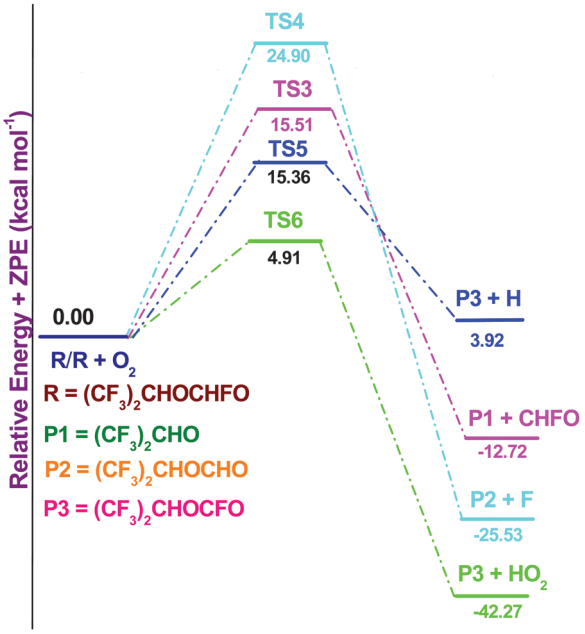

Fig. 3 Schematic potential energy diagram for the thermal decomposition and oxidation pathways of $(CF_3)_2CHOCHFO$ radicals at the M06-2X/6-311++G(d,p) + ZPE level. All values are given in kcal mol^{-1}.

per unit volume respectively. ΔE, k_B and h are the barrier height including ZPE, Boltzmann's and Planck's constants, respectively. Barrier heights, ΔE, obtained from the M06-2X/6-311++G(d,p) level are used in rate constant calculations. Calculation for the tunneling correction factor $\Gamma(T)$ was made using Wigner's empirical formula.[50] The partition functions for the respective transition states and reactants at 298 K are obtained under the rigid rotor, harmonic oscillator approximations and from the data calculated at the M06-2X/6-31+G(d,p) level. However, the hindered-rotor approximation of Chuang and Truhlar[51] was used for calculating the partition function of lower vibration modes. It has been observed that H-abstraction by the OH radical proceeds *via* a two step mechanism. The first step involves formation of the pre-reactive complexes (RCs) with pre-equilibrium rate constants (K_{eq}) and the second step yields the corresponding radical and water with the rate constant $k_2^{\dagger}$. The overall rate constant including equilibrium constant (K_{eq}) and rate constant $\left(k_2^{\dagger}\right)$ are given by,

$$K_{eq} = \frac{Q_{RC}}{Q_A \cdot Q_B} e^{(E_R - E_{RC})/RT} \quad (10)$$

and $k_2^{\dagger}$ can be obtained from TST in the form

$$k_2^{\dagger} = \sigma\Gamma(T)\frac{k_B T}{h}\frac{Q_{TS}}{Q_{RC}} e^{-(E_{TS} - E_{RC})/RT} \quad (11)$$

The rate constant for H-abstraction *via* reactions (1–2) are then obtained by the following expression,

$$k = K_{eq} \times k_2^{\dagger} = \sigma\Gamma(T)\frac{k_B T}{h}\frac{Q_{TS}}{Q_A \cdot Q_B} e^{-(E_{TS} - E_R)/RT} \quad (12)$$

where, Q_A, Q_B, Q_{RC} and Q_{TS} represent the total partition functions (per unit volume) of the reactants, reaction complexes and

transition states, respectively. E_{TS}, E_{RC} and E_R are the total energies (ZPE corrected) of transition states, reaction complexes and reactants, respectively. Thus it seems that the final expression (eqn (12)) for estimating the rate constant and barrier height turns out to be the usual CTST expression (eqn (9)) used for the determination of the rate constant and barrier height of a direct reaction, irrespective of the energy of pre-reactive reactant complexes (RC1, RC2a and RC2b). However, the formation of pre- and post reaction complexes affects the tunneling factor by modifying the shape of the potential energy surface and changes the tunneling factor to some extent. In the calculation of reactant electronic partition function, the excited state of the OH radical is included, with a 140 cm^{-1} splitting due to spin–orbit coupling.

The calculated rate constant values in the temperature range of 250–1000 K are listed in Table 3 and also plotted in Fig. 4 along with the available experimental values. The rate constant for the H atom abstraction reaction of $(CF_3)_2CHOCH_2F$ by the OH radical for reactions 1 and 2 are calculated to be $k_1 = 1.64 \times 10^{-14}$ and $k_2 = 2.04 \times 10^{-14}$ cm^3 $molecule^{-1}$ s^{-1}, respectively, at 298 K. It gives a total rate constant value of $k_{OH} = 3.68 \times 10^{-14}$ cm^3 $molecule^{-1}$ s^{-1} which is in good agreement with the experimental value of $(3.9 \pm 0.3) \times 10^{-14}$ cm^3 $molecule^{-1}$ s^{-1} at 298 K reported by Andersen *et al.*[17] Moreover, our calculated rate constant values agree quite well in the temperature range of the available experimental data indicating the reliability of our calculation for this reaction. The calculated rate constant values at 298 K show that H-abstraction from the $-CH_2F$ site has greater contribution to the total rate constant than that from the $-CH(CF_3)_2$ of the Sevoflurane molecule and the relative contribution of the former site increases further with the increase in temperature. For example, the contribution of the $-CH_2F$ site to the total rate constant becomes almost 11 times greater than the contribution of the $-CH(CF_3)_2$ site at 1000 K. This result is in accord with the mechanism proposed by Andersen *et al.*[17] which is based on his experimental observation that atmospheric oxidation of Sevoflurane initiated by OH radicals and Cl atoms proceeds with the abstraction of a H-atom from the $-CH_2F$ end of the molecule and the resulting products retained the H-atom from the $(CF_3)_2CHO$ site.

Table 3 Rate coefficient values (in cm^3 $molecule^{-1}$ s^{-1}) for hydrogen abstraction reactions of $(CF_3)_2CHOCH_2F$ with OH radicals and total rate coefficient (k_{OH}) values as calculated at the M06-2X/6-311++G(d,p) level

Temp. range	M06-2X				
T (K)	$k_{TS1} \times 10^{14}$	$k_{TS2a} \times 10^{14}$	$k_{TS2b} \times 10^{14}$	$k_{TS2} \times 10^{14}$	$k_{OH} \times 10^{14}$
250	1.24	1.18	0.13	1.31	2.55
298	1.64	1.63	0.42	2.05	3.68
300	1.65	1.64	0.43	2.07	3.74
350	2.11	2.17	1.06	3.23	5.35
400	2.62	2.78	2.18	4.96	7.59
450	3.19	3.48	4.01	7.49	10.69
500	3.85	4.27	6.78	11.05	14.91
550	4.59	5.18	10.77	15.95	20.55
600	5.43	6.19	16.30	22.49	27.93
650	6.37	7.33	23.72	31.05	37.43
700	7.42	8.60	33.41	42.01	49.43
750	8.59	9.99	45.78	55.77	64.36
800	9.87	11.53	61.27	72.8	82.67
850	11.29	13.20	80.35	93.55	104.8
900	12.83	15.02	103.5	118.52	131.4
950	14.51	16.99	131.3	148.29	162.8
1000	16.33	19.12	164.2	183.32	199.6

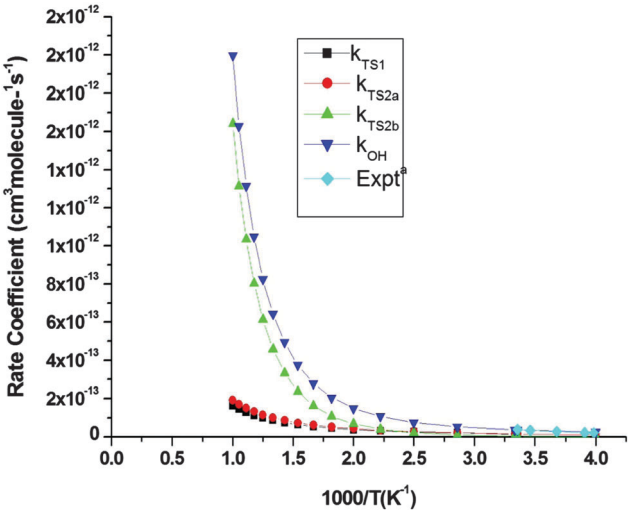

Fig. 4 Rate constants for hydrogen abstraction reactions of $(CF_3)_2CHOCH_2F$ with OH radicals and total rate constant (k_{OH}) for the $(CF_3)_2CHOCH_2F$ + OH reactions. [a] Ref. 17 (*J. Phys. Chem. A*, 2012, **116**, 5806).

Owing to non-Arrhenius behavior due to tunneling and existence of multiple channels, the temperature variation of the rate constant for this type of reaction is generally expressed by a three parameter model equation:

$$k(T) = AT^n \exp(-\Delta E^0/RT) \quad (13)$$

where A, n and ΔE^0 are the adjustable parameters to obtain best fitting. The activation energy can be obtained from the expression:

$$E_a = \Delta E^0 + nRT \quad (14)$$

Our calculated rate constants (k_{OH}) in the temperature range 250–1000 K is seen to be best described by the following model equation:

$$k_{OH} = 1.33 \times 10^{-27} T^{4.94} \exp(832/T) \quad (15)$$

The activation energy estimated from eqn (14) at 298 K is 1.27 kcal mol^{-1}.

D. Atmospheric implications

i. Atmospheric lifetime. The lifetime of inhaled anaesthetics in the atmosphere is thought to depend almost completely on the reaction with hydroxyl radicals.[10] In general, the tropospheric lifetime (τ_{eff}) of $(CF_3)_2CHOCH_2F$ can be estimated by assuming that its removal from the troposphere occurs mainly through the reactions with OH radicals. Then (τ_{eff}) can be expressed as[52]

$$\tau_{eff} \approx \tau_{OH}$$

However, this equation does not take into consideration the errors due to the vertical temperature profile of the troposphere.

When calculating OH-based lifetimes, the use of 272 K as an average tropospheric temperature and methyl chloroform (CH_3CCl_3), as a chemical of well known source and sink, has been suggested[53] to minimize the errors resulting from neglecting the specific temperature dependences. Thus, lifetime estimations for HFEs are generally calculated on the basis of gas-phase removal by OH only and with methyl chloroform (MCF) as the reference:

$$\tau_{OH}^{Sevo} = \frac{k_{MCF}(272\ K)}{k_{Sevo}(272\ K)}\tau_{OH}^{MCF}$$

where τ_{OH}^{Sevo} is the lifetime for Sevoflurane, k_{Sevo} and k_{MCF} are the rate constants for the reactions of OH radicals with Sevoflurane and methyl chloroform (MCF), respectively, at T = 272 K and τ_{OH}^{MCF} = 5.99 years.[53] Taking the values of rate constants for $k_{MCF} = 6.14 \times 10^{-15}$ from ref. 53 and the calculated rate constant of Sevoflurane $k_{Sevo} = 3.03 \times 10^{-14}$ cm^3 $molecule^{-1}$ s^{-1}, at 272 K, the estimated lifetime is found to be 1.2 years which is in agreement with the reported value of 2.2 years[20] and 1.8 years.[12]

ii. Global warming potentials (GWPs). Global-warming potential (GWP)[54] is a relative measure of how much heat a greenhouse gas traps in the atmosphere. The global warming potential is generally predicted based on the time-integrated radiative efficiency from the instantaneous emission of 1 kg of a compound relative to that of 1 kg of a reference gas (CO_2). It can be expressed as an absolute GWP for a gas i ($AGWP_i$) or as a dimensionless value by dividing the $AGWP_i$ by the AGWP of a reference gas (CO_2). Here, GWPs for hydrofluoroethers are estimated (relative to CO_2) using the expression given by Hodnebrog *et al.*[20] as:

$$GWP_i(H) = \frac{\int_0^H RF_i(t)dt}{\int_0^H RF_{CO_2}(t)dt} = \frac{AGWP_i(H)}{AGWP_{CO_2}(H)}$$

If A_i is the radiative forcing efficiency (RE in W m^{-2} ppb^{-1}), τ_i is the lifetime for a gas i and H is the time horizon, then assuming that its removal from the atmosphere can be represented by exponential decay, the integrated radiative forcing efficiency up to H is taken as:[20]

$$AGWP_i(H) = A_i\tau\left(1 - \exp\left(-\frac{H}{\tau}\right)\right).$$

To obtain theoretical estimation of RE for Sevoflurane, the infrared intensities and the wave numbers of harmonic vibrational modes were obtained at the B3LYP/6-31G** level of theory as suggested by Bravo *et al.*[55,56] The calculated vibrational wave numbers were then scaled using the expression $\bar{\nu}_{scal} = 0.977\bar{\nu}_{calc} + 11.664$ cm^{-1} as suggested by Bravo *et al.*,[55] so that calculated vibrational modes can be related to the positions of the important experimental absorption bands. Using data from the same level of theory and the method outlined by Pinnock *et al.*,[57] the radiative efficiency of HFE molecules was calculated using the relationship:

$$RE = \sum_k A_k F(\bar{\nu}_k)$$

where A_k is the absorption cross-section in cm^2 $molecule^{-1}$ averaged over a 10 cm^{-1} interval around the wave number ($\bar{\nu}_k$) and $F(\bar{\nu}_k)$ is the instantaneous, cloudy sky, radiative forcing per unit cross section per wave number (W m^{-2} cm $(cm^2\ molecule^{-1})^{-1}$) evaluated at the band scaled center wave number ($\bar{\nu}_k$). It is known that REs derived from the Pinnock *et al.*[57] method are within 10% of those obtained from the more detailed models.[55] Table 4 provides the tropospheric lifetime, radiative efficiency and GWPs value of 100 year time horizon for Sevoflurane along with the available reported results. Our computed GWP value of 132 is in good agreement with the reported value of 106 by Ryan and Nielsen[10] and 130 by Andersen *et al.*[17] Our calculated radiative efficiency value of 0.337 W m^{-2} ppb^{-1} is also seen to be in good agreement with the literature value of 0.351 W m^{-2} ppb^{-1} reported by Andersen *et al.*[17]

Table 4 Atmospheric lifetime of Sevoflurane at 272 K and its GWPs at 298 K estimated using the results from B3LYP/6-31G** level

Atmospheric lifetime (years)	Radiative efficiencies (W m^{-2} $ppbv^{-1}$)	Global warming potentials w.r.t. CO_2 for a 100 year time horizon	Ref.
1.1	0.351	130	Andersen *et al.*[17]
1.8	0.351	210	Andersen *et al.*[12]
1.2	0.365	106	Ryan and Nielsen[10]
4.0	—	218	Langbein *et al.*[8]
1.2	0.337	132	This work

iii. Fate of fluorinated ester. It is well known that fluorinated esters (FESs) are the primary products of the atmospheric oxidation of hydrofluoroethers.[58] Like HFEs, FESs also undergo photochemical oxidation in the troposphere with atmospheric oxidants, OH radicals or Cl atoms. However, recent studies have also shown that wet deposition might not be an important sink for all FESs and the OH radicals are the most dominant oxidant.[59,60] In the present study we also study the OH radical and Cl-atom initiation hydrogen abstraction reaction from $(CF_3)_2CHOC(O)F$. The optimized geometries of two transition states (TS9 and TS10) are shown in Fig. S1 in ESI.† The calculated barrier heights for hydrogen abstraction by OH-radicals and Cl atoms are found to be 4.22 and 8.12 kcal mol^{-1}, respectively. This suggests that OH-initiated hydrogen abstraction of $(CF_3)_2CHOCFO$ is the dominant pathway. However, further detailed studies are required for OH and Cl initiated degradation of ester to determine the atmospheric fate of it and can be a subject for further work.

IV Conclusions

The potential energy surface and reaction kinetics for the Sevoflurane + OH reactions are investigated at the M06-2X/6-31+G(d,p) level of theory. The hydrogen abstraction reactions of Sevoflurane with OH radicals proceed by a complex indirect mechanism involving the formation of reactant complexes in the entrance channel and product complexes in the exit channel. The barrier heights for dominant reaction pathways calculated at the M06-2X/6-311++G(d,p) level are found to be 1.42 kcal mol^{-1}. The thermal rate constant for the H atom abstraction of $(CF_3)_2CHFOCH_2F$ by OH radicals is found to be 3.68×10^{-14} cm^3 $molecule^{-1}$ s^{-1},

respectively, at 298 K which is in very good agreement with the available experimental data. Our calculations suggest that the H abstraction from the $-CH_2F$ group is kinetically and thermodynamically more favorable than the –CH group attached to two $-CF_3$ groups for OH reactions. The $\Delta_f H^o_{298}$ values for $(CF_3)_2CHOCH_2F$, $(CF_3)_2COCH_2F$ and $(CF_3)_2CHOCHF$ radicals calculated from M06-2X/6-311++G(d,p) results are predicted to be −414.81, −364.36 and −364.57 kcal mol^{-1}, respectively. The atmospheric lifetime and GWPs at a 100 year horizon of Sevoflurane are estimated to be 1.2 years and 132, respectively. The atmospheric fate of thermal decomposition of $(CF_3)_2CHOCHFO$ radicals is investigated at the M06-2X/6-31+G(d,p) level of theory. Our results reveal that the most dominant decomposition pathway for $(CF_3)_2CHOCHFO$ radical is the reaction with O_2 that occurs with a barrier height of 4.91 kcal mol^{-1} as obtained from the M06-2X/6-311++G(d,p) method. The dominance of oxidative pathways in the decomposition of $(CF_3)_2CHOCHFO$ radicals established during the present investigation is in accord with the results obtained by Andersen *et al.*[17] The present results provide assistance for understanding the experimentally observed fate of thermal decomposition and oxidation of the title alkoxy radical.

Acknowledgements

The authors acknowledge financial support from the Department of Science and Technology, New Delhi, in the form of a project (SR/NM.NS-1023/2011(G)). BKM is thankful to University Grants Commission, New Delhi, for providing Dr D. S. Kothari Post-doctoral Fellowship. AKC acknowledges CSIR, India, for financial assistance through project no. 01(2494)/11/EMR-II. DB is thankful to Council of Scientific and Industrial research, New Delhi, for providing Junior Research Fellowship. We are also thankful to the learned reviewers for their constructive suggestions in improving the quality of the manuscript.

References

1 M. J Molina and F. S. Rowland, *Nature*, 1974, **249**, 810.
2 J. D. Farman, B. G. Gardiner and J. D. Shanklin, *Nature*, 1985, **315**, 207.
3 W. T. Tsai, *J. Hazard. Mater.*, 2005, **119**, 69.
4 A. Sekiya and S. Misaki, *J. Fluorine Chem.*, 2000, **101**, 215.
5 A. R. Ravishankara, A. A. Turnipseed, N. R. Jensen, S. Barone, M. Mills, C. J. Howark and S. Solomon, *Science*, 1994, **263**, 71.
6 W. Zierkiewicz, D. Michalska and T. Zeegers-Huyskens, *Phys. Chem. Chem. Phys.*, 2010, **12**, 13681.
7 J. Lerman, N. Sikich, S. Kleinman and S. Yentis, *Anesthesiology*, 1994, **80**, 814.
8 T. Langbein, H. Sonntag, D. Trapp, A. Hoffmann, W. Malms, E.-P. Roth, V. Mors and R. Zellner, *Br. J. Anaesth.*, 1999, **82**, 66.
9 Y. Shiraishi and K. Ikeda, *J. Clin. Anesth.*, 1990, **2**, 381.
10 S. M. Ryan and C. J. Nielsen, *Anesth. Analg.*, 2010, **111**, 92.
11 K. P. Shine, *Br. J. Anaesth.*, 2010, **105**, 731.
12 M. P. Sulbaek Andersen, S. P. Sander, O. J. Nielsen, D. S. Wagner, T. J. Sanford, Jr. and T. J. Wallington, *Br. J. Anaesth.*, 2010, **105**, 760.
13 C. J. Young and J. L. Apfelbaum, *J. Clin. Anesth.*, 1995, **7**, 564.
14 I. Bravo, A. Rodriguez, D. Rodriguez, Y. Diaz-de-Mera, A. Notario and A. Aranda, *ChemPhysChem*, 2013, **14**, 3834.
15 W. Zierkiewicz, *Chem. Phys. Lett.*, 2013, **555**, 72.
16 A. C. Brown, C. E. Canosa-Mas, A. D. Parr, J. M. T. Pierce and R. P. Wayne, *Nature*, 1989, **341**, 635.
17 M. P. Sulbaek Andersen, O. J. Nielsen, B. Karpichev, T. J. Walllington and S. P. Sander, *J. Phys. Chem. A*, 2012, **116**, 5806.
18 L. Chen, S. Kutsuna, K. Tokuhashi, A. Sekiya, R. Tamai and Y. Hibino, *J. Phys. Chem. A*, 2005, **109**, 4766.
19 United Nations Environment Programme Ozone Secretariat, http://ozone.unep.org/Assessment_Panels/SAP/Scientific_Assessment_2010/.
20 Ø. Hodnebrog, M. Etminan, J. S. Fuglestvedt, G. Marston, G. Myhre, C. J. Nielsen, K. P. Shine and T. J. Wallington, *Rev. Geophys.*, 2013, **51**, 300.
21 J. J. Orlando, G. S Tyndall and T. J. Wallington, *Chem. Rev.*, 2003, **103**, 4657.
22 H. J. Singh and B. K. Mishra, *J. Mol. Model.*, 2011, **17**, 415.
23 H. J. Singh and B. K. Mishra, *J. Mol. Model.*, 2010, **16**, 1473.
24 H. J. Singh, B. K. Mishra and P. K. Rao, *Can. J. Chem.*, 2012, **90**, 403.
25 H. J. Singh and B. K. Mishra, *J. Chem. Sci.*, 2011, **123**, 733.
26 H. J. Singh, B. K. Mishra and N. K. Gour, *Theor. Chem. Acc.*, 2010, **125**, 57.
27 M. J. Frisch, G. W. Trucks, H. B. Schlegel, G. E. Scuseria, M. A. Robb, J. R. Cheeseman, J. A. Montgomery Jr., T. Vreven, K. N. Kudin, J. C. Burant, J. M. Millam, S. S. Iyengar, J. Tomasi, V. Barone, B. Mennucci, M. Cossi, G. Scalmani, N. Rega, G. A. Petersson, H. Nakatsuji, M. Hada, M. Ehara, K. Toyota, R. Fukuda, J. Hasegawa, M. Ishida, T. Nakajima, Y. Honda, O. Kitao, H. Nakai, M. Klene, X. Li, J. E. Knox, H. P. Hratchian, J. B. Cross, C. Adamo, J. Jaramillo, R. Gomperts, R. E. Stratmann, O. Yazyev, A. J. Austin, R. Cammi, C. Pomelli, J. W. Ochterski, P. Y. Ayala, K. Morokuma, G. A. Voth, P. Salvador, J. J. Dannenberg, V. G. Zakrzewski, S. Dapprich, A. D. Daniels, M. C. Strain, O. Farkas, D. K. Malick, A. D. Rabuck, K. Raghavachari, J. B. Foresman, J. V. Ortiz, Q. Cui, A. G. Baboul, S. Clifford, J. Cioslowski, B. B. Stefanov, G. Liu, A. Liashenko, P. Piskorz, I. Komaromi, R. L. Martin, D. J. Fox, T. Keith, M. A. Al-Laham, C. Y. Peng, A. Nanayakkara, M. Challacombe, P. M. W. Gill, B. Johnson, W. Chen, M. W. Wong, C. Gonzalez and J. A. Pople, *Gaussian09, Revision B.01*, Gaussian, Inc., Wallingford CT, 2010.
28 Y. Zhao and D. G. Truhlar, *Theor. Chem. Acc.*, 2008, **120**, 215.
29 N. K. Gour, R. C. Deka, H. J. Singh and B. K. Mishra, *J. Fluorine Chem.*, 2014, **160**, 64.
30 G. Srinivasulu and B. Rajakumar, *J. Phys. Chem. A*, 2013, **117**, 4534.

31 T. C. Dinadayalane, G. Paytakov and J. Leszczynski, *J. Mol. Model.*, 2013, **19**, 2855.
32 M. R. Dash and B. Rajakumar, *Atmos. Environ.*, 2013, **79**, 161.
33 M. Lily, B. K. Mishra and A. K. Chandra, *J. Fluorine Chem.*, 2014, **161**, 51.
34 D. Mandal, K. Sen and A. K. Das, *J. Phys. Chem. A*, 2012, **116**, 8382.
35 L. Sandhiya, P. Kolandaivel and K. Senthilkumar, *Struct. Chem.*, 2012, **23**, 1475.
36 C. Gonzalez and H. B. Schlegel, *J. Chem. Phys.*, 1989, **90**, 2154.
37 M. P. Freitas, M. Buhl, D. O. Hagan, R. A. Cormanich and C. F. Tormena, *J. Phys. Chem. A*, 2012, **116**, 1677.
38 A. Lesarri, A. Vega-Toribio, R. D. Suenram, D. J. Brugh and J. U. Grabow, *Phys. Chem. Chem. Phys.*, 2010, **12**, 9624.
39 P. Tang, I. Zubryzcki and Y. Xu, *J. Comput. Chem.*, 2001, **22**, 436.
40 H. J. Singh, N. K. Gour, P. K. Rao and L. Tiwari, *J. Mol. Model.*, 2013, **19**, 4815.
41 A. Beste and A. C. Buchanan, III, *Chem. Phys. Lett.*, 2012, **550**, 19.
42 J. M. Younker, A. Beste and A. C. Buchanan, III, *Chem. Phys. Lett.*, 2012, **545**, 100.
43 T. Elder, *Energy Fuels*, 2013, **27**, 4785.
44 A. Beste and A. C. Buchanan, III, *Energy Fuels*, 2010, **24**, 2857.
45 K. J. Devi and A. K. Chandra, *Chem. Phys. Lett.*, 2011, **502**, 23.
46 M. W. Chase Jr., NIST-JANAF Thermochemical Tables, *J. Phys. Chem. Ref. Data*, 1998, **9**, 1.
47 H. Gao, Y. Wang, S. Wang, J. Y. Liu and C.-C. Sun, *THEOCHEM*, 2009, **913**, 107.
48 D. R. Lide, *CRC Handbook of Chemistry and Physics*, CRC Press, New York, 89th edn, 2009.
49 D. G. Truhlar, B. C. Garrett and S. J Klippenstein, *J. Phys. Chem.*, 1996, **100**, 12771.
50 E. P. Wigner, *Z. Phys. Chem.*, 1932, **B19**, B203.
51 Y. Y. Chuang and D. G. Truhlar, *J. Chem. Phys.*, 2000, **112**, 1221.
52 M. J. Kurylo and V. L. Orkin, *Chem. Rev.*, 2003, **103**, 5049.
53 C. M. Spivakovsky, J. A. Logan, S. A. Montzka, Y. J. Balkanski, M. Foreman-Fowler, D. B. A. Jones, L. W. Horowitz, A. C. Fusco, C. A. M. Brenninkmeijer, M. J. Prather, S. C. Wofsy and M. B. McElroy, *J. Geophys. Res.*, 2000, **105**(D7), 8931.
54 J. K. Hammitt, A. K. Jain, J. L. Adams and D. J. Wuebbles, *Nature*, 1996, **381**, 301.
55 I. Bravo, A. Aranda, M. D Hurley, G. Marston, D. R Nutt, K. P Shine, K. Smith and T. J. Wallington, *J. Geophys. Res.*, 2010, **115**, D24317.
56 I. Bravo, G. Marston, D. R. Nutt and K. P. Shine, *J. Quant. Spectrosc. Radiat. Transfer*, 2011, **112**, 1967.
57 S. Pinnock, M. D. Hurley, K. P. Shine, T. J. Wallington and T. J. Smyth, *J. Geophys. Res.*, 1995, **100**, 23227.
58 I. Bravo, Y. Diaz-de-Mera, A. Aranda, K. Smith, K. P. Shine and G. Marstond, *Phys. Chem. Chem. Phys.*, 2010, **12**, 5115.
59 L. Chen, S. Kutsuna, K. Tokuhashi and A. Sekiya, *Chem. Phys. Lett.*, 2004, **400**, 56.
60 S. Kutsuna, L. Chen, K. Ohno, K. Tokuhashi and A. Sekiya, *Atmos. Environ.*, 2004, **38**, 725.

